RESEARCH

Transcriptomic landscape of radiation-induced murine thyroid proliferative lesions

Elena Stauffer[1], Peter Weber[1], Theresa Heider[1], Claudia Dalke[2], Andreas Blutke[3], Axel Walch[3], Gerald Burgstaller[4], Nikko Brix[5], Kirsten Lauber[5,6], Horst Zitzelsberger[1,6], Kristian Unger[1,5,6] and **Martin Selmansberger[1]**

[1]Helmholtz Zentrum München – German Research Center for Environmental Health, Research Unit Radiation Cytogenetics, Neuherberg, Germany
[2]Helmholtz Zentrum München – German Research Center for Environmental Health, Institute of Metabolism and Cell Death, Neuherberg, Germany
[3]Helmholtz Zentrum München – German Research Center for Environmental Health, Research Unit Analytical Pathology, Neuherberg, Germany
[4]Helmholtz Zentrum München – Institute of Lung Biology and Disease (ILBD) and Comprehensive Pneumology Center (CPC), Member of the German Center for Lung Research (DZL), Munich, Germany
[5]Department of Radiation Oncology, University Hospital, LMU Munich, Munich, Germany
[6]Helmholtz Zentrum München – German Research Center for Environmental Health GmbH, Clinical Cooperation Group 'Personalized Radiotherapy in Head and Neck Cancer', Neuherberg, Germany

Correspondence should be addressed to M Selmansberger: martin.selmansberger@helmholtz-muenchen.de

Abstract

Thyroid carcinoma incidence rates in western societies are among the fastest rising, compared to all malignant tumors over the past two decades. While risk factors such as age and exposure to ionizing radiation are known, early-state carcinogenic processes or pre-lesions are poorly understood or unknown. This study aims at the identification and characterization of early-state radiation-associated neoplastic processes by histologic and transcriptomic analyses of thyroid tissues derived from a mouse model. Comprehensive histological examination of 246 thyroids (164 exposed, 82 non-exposed) was carried out. Proliferative and normal tissues from exposed cases and normal tissue from non-exposed cases were collected by laser-capture microdissection, followed by RNAseq transcriptomic profiling using a low input 3′-library preparation protocol, differential gene expression analysis and functional association by gene set enrichment analysis. Nine exposed samples exhibited proliferative lesions, while none of the non-exposed samples showed histological abnormalities, indicating an association of ionizing radiation exposure with histological abnormalities. Activated immune response signaling and deregulated metabolic processes were observed in irradiated tissue with normal histology compared to normal tissue from non-exposed samples. Proliferative lesions compared to corresponding normal tissues showed enrichment for mainly proliferation-associated gene sets. Consistently, proliferative lesion samples from exposed mice showed elevated proliferation-associated signaling and deregulated metabolic processes compared to normal samples from non-exposed mice. Our findings suggest that a molecular deregulation may be detectable in histologically normal thyroid tissues and in early proliferative lesions in the frame of multi-step progression from irradiated normal tissue to tumorous lesions.

Key Words

- thyroid pathogenesis
- thyroid carcinogenesis
- thyroid neoplasia
- histology
- transcriptomics

Endocrine-Related Cancer (2021) **28**, 213–224

https://erc.bioscientifica.com
https://doi.org/10.1530/ERC-21-0019

Introduction

Incidence rates for thyroid cancer increased worldwide over the last decades, thus becoming the most common endocrine malignancy (La Vecchia *et al.* 2015). While environmental and lifestyle factors and the effect of overdiagnosis due to improved screening methods are discussed, their impact on the increased incidence rates remains to be proved (Wiltshire *et al.* 2016). Despite the high incidence rates, thyroid cancer, especially the papillary thyroid carcinoma (PTC) subtype, is associated with a good prognosis after radical surgery and shows low mortality rates (La Vecchia *et al.* 2015).

Exposure to ionizing radiation at young age, both internal and external, is a well-known risk factor for the development of thyroid carcinoma (Ron *et al.* 1995). Ionizing radiation exposure in childhood greatly increases the risk for thyroid cancer, particularly PTC. Numerous studies have shown that after the Chernobyl reactor accident and the resulting radiation exposure of the population through radioactive fallout (including I-131), the incidence rate of thyroid carcinomas has significantly increased (Kazakov *et al.* 1992, Nikiforov 2006, Cahoon *et al.* 2017, Efanov *et al.* 2018).

Thyroid carcinomas can develop either from follicular cells or c-cells. The resulting malignancies are classified into medullary carcinomas (c-cells) or papillary, follicular and anaplastic carcinomas (follicular cells). Papillary carcinomas are further divided into different subtypes based on the predominant histological architecture (Xing 2013). The majority of thyroid cancer originates from follicular cells, such as PTC and follicular thyroid carcinoma (FTC) (DeLellis 2004, Baloch & LiVolsi 2018). While it is proposed that FTC evolves from follicular adenoma (FA), papillary thyroid carcinoma has no benign precursor lesion (Sponziello *et al.* 2013).

Mouse models are frequently used to study thyroid cancer and the underlying carcinogenic processes. However, although mouse and human thyroid cancers show biological similarities, they greatly differ in histological characteristics. In contrast to human thyroid cancer, murine histological cancer entities are not distinguished, for example, the follicular carcinoma has only a papillary pattern but is classified as follicular carcinoma (Boorman 1995, Capen 2001).

As for other cancer types, a series of genetic and epigenetic alterations is responsible for the initiation and progression of thyroid cancer according to a multi-step model (Vogelstein & Kinzler 1993, Kondo *et al.* 2006). Those alterations, that consequently stimulate effectors of the MAPK signaling pathway or PI3K/AKT signaling pathway, play a central role in thyroid carcinogenesis (Nikiforova & Nikiforov 2008). Point mutation of the BRAF and RAS genes and rearrangements of the RET gene are common in PTC, while the rearrangements of PAX8/PPARy are mostly prevalent in FTC and FTA (Xing 2005, Nikiforov & Nikiforova 2011). The detection of genetic alterations in follicular adenoma, which can be considered as early lesions, support the concept of a multi-step carcinogenesis model. However, it remains unclear at what point follicle cells develop proliferative potential (Jung *et al.* 2016). Additionally, a cancer stem cell carcinogenic model and a fetal cell carcinogenesis model are currently discussed as alternatives to the multi-step process (Zane *et al.* 2016).

Nowadays, molecular alterations in thyroid cancer are well characterized, while early state events or precursor lesions still remain poorly understood or are unknown (Xing 2013, Ye *et al.* 2017). Besides genetic aberrations such as RET- and PAX8-rearrangements and BRAF V600E mutations, epigenetic modifications including silencing of RASSF1A via promoter methylation and post-transcriptional regulation via miRNAs and lncRNAs in thyroid carcinogenesis were recently investigated (Brown *et al.* 2014, Colamaio *et al.* 2015, Sedaghati & Kebebew 2019).

The aim of this study was the identification and characterization of molecular processes in the early stages of the carcinogenic processes in the thyroid. For this purpose, we used a mouse model and performed comprehensive histological analyses of thyroids from a cohort of mice that received low-dose gamma-irradiation early in life. Subsequently, laser capture microdissection (LCM) enabled transcriptomic profiling of histologically normal and aberrant tissue areas, in order to gain further insight in early events of genetic and molecular deregulation that may drive the early phases of thyroid malignancies.

Material and methods

Workflow

The entire workflow of this study is visualized in Fig. 1.

Thyroid tissues

Mouse thyroids were obtained from the INSTRA lifetime study and details on mice are presented in Dalke *et al.* (2018).

https://erc.bioscientifica.com
https://doi.org/10.1530/ERC-21-0019

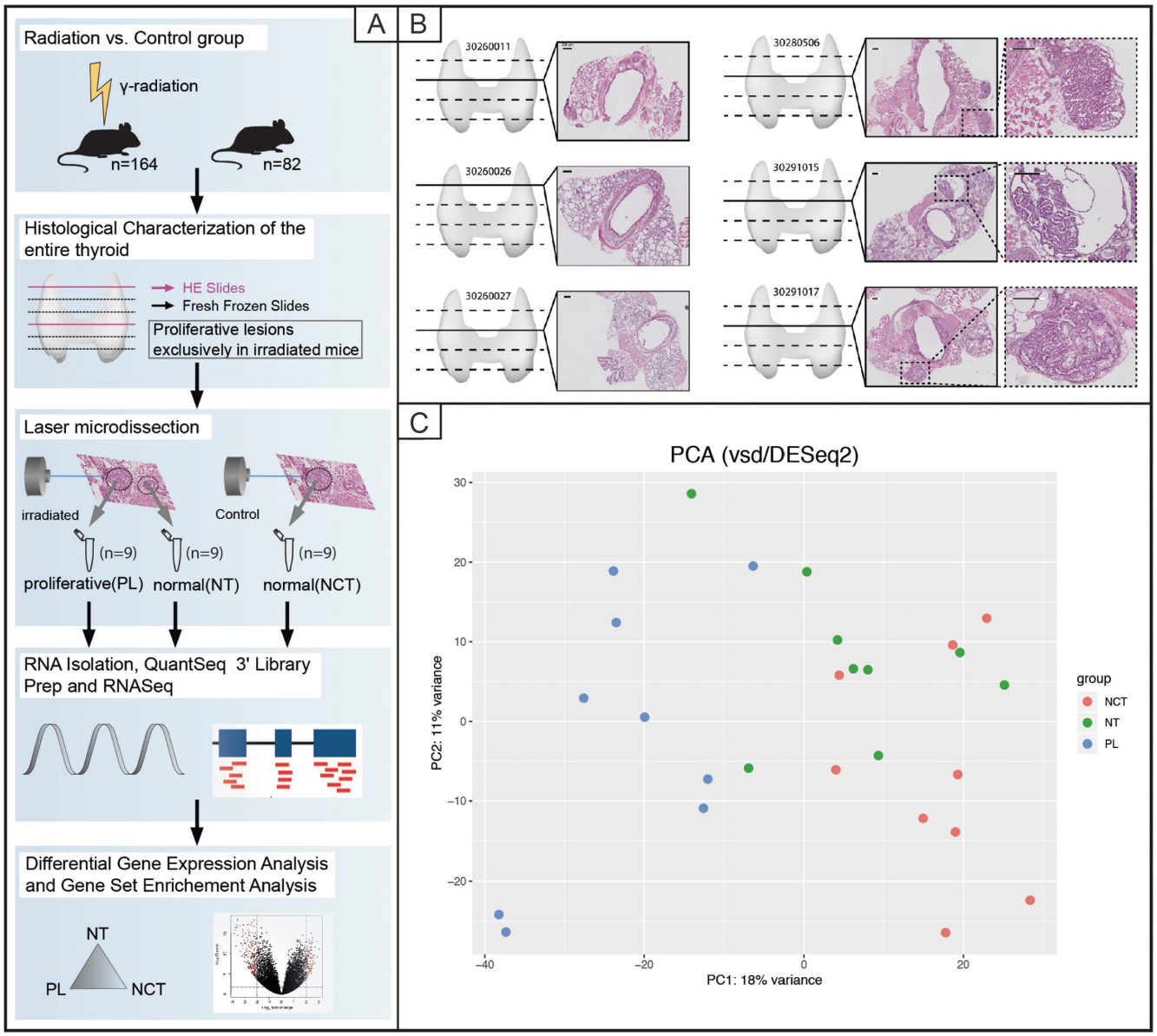

Figure 1
Panel A: Workflow of the study. Panel B: Examples of thyroid HE-sections and histological examination (all samples in Supplementary Fig. 1). Panel C: Principal component analysis of RNAseq data (vst counts) generated from the three histological groups. A full color version of this figure is available at https://doi.org/10.1530/ERC-21-0019.

One hundred sixty-four mice were whole body irradiated at the age of 10 weeks with different doses of 0.063, 0.125 and 0.5 Gy. Eighty-two mice exposed to 0 Gy served as control group (sham irradiation). Animals were sacrificed at pre-determined time points (6, 12, 18, 24 months) and thyroids were collected. Details of all mice and histopathologically examined samples are shown in Supplementary Table 1 (see section on supplementary materials given at the end of this article), and samples analyzed by RNAseq are shown in Supplementary Table 2. Approximately 50% of the mice included in the study harbor a heterozygous mutation of the ERCC2 gene. This mutation was investigated for its potential to promote eye lens cataracts after exposure to ionizing radiation in a previous study, while explicitly no association of thyroid aberrations and ERCC2 gene mutation was reported. The study also provides a detailed description of the genomic background of these mice (Dalke *et al.* 2018).

Tissue processing and comprehensive histological examination

Tissues were snap-frozen in liquid nitrogen upon resection and embedded in a Cryo Gel (Leica Surgipath Cryogel) before transversal sectioning. A total number of 246 thyroids were exhaustively processed into 30 and 12 µm tissue sections. While the series of 30 µm sections were kept for potential laser capture microdissection (LCM), the 12 µm sections were stained with hematoxylin and eosin (HE) for histopathological evaluation. Dependent on the size, 10–20 thyroid sections were analyzed histopathologically. The sections were independently examined by two pathologists (A W and A B). All thyroid samples were investigated and classified based on the WHO criteria for the evaluation of murine thyroid tumors and according to the international classification of rodent tumors (Jokinen & Botts 1994, Capen 2001, DeLellis 2004). Normal thyroid tissues were classified by variable-sized follicles covered by monolayers of flattened epithelial cells. Further, hyperplastic thyroid tissues were diagnosed by the occurrence of small follicles showing scant colloid and tall epithelial cells adjacent to normal follicles. In contrast, neoplastic thyroid lesions such as adenomas were identified by the presence of demarcated histologic areas with a distinct follicular and/or papillary architecture. To differentiate those neoplastic lesions from carcinomas, the invasion of the surrounding glandular parenchyma or stroma was evaluated. Due to the absence of such invasive areas, there was no indication for carcinomas of the papillary or follicular subtype in any of the neoplastic cases. Furthermore, the presence of immune cells was quantitatively assessed in the evaluated HE slides. Immune cell infiltration was expressed as the number of immune cells per section area (cells/mm^2) and was determined intwo to three sections per case. After histological analysis, two groups of tissue samples were defined: the first group comprised proliferative lesions from the irradiated mice, and the second group contained morphologically normal tissue taken from the same animal, respectively. A third group of normal thyroid tissues from sex- to age-matched non-irradiated mice was added. For molecular investigation 30 µm thick sections were prepared for LCM. LCM was carried out utilizing a PALM MicroBeam device (Zeiss), which allows the dissection and collection of targeted tissue formations or groups of cells after microscopic identification, according to the manufacturers protocol and as previously described (Morrogh *et al.* 2007).

The histological findings in irradiated and non-irradiated mice were statistically analyzed by Fisher's exact test. Immune cell scores were compared between the three groups by the ANOVA and pair-wise compared by *post hoc* Tukey test. Statistical significance was considered at $P < 0.05$.

RNA isolation and RNAseq 3′library preparation

The RNA extraction from the laser capture microdissected cells was performed with the RNeasy Micro Kit (Qiagen), according to the manufacturer's protocol. RNA quality was evaluated using a Bioanalyzer 2100 Systems (Agilent Technologies, Inc.) with Agilent RNA 6000 Pico Kit (#5067-1513, Agilent Technologies, Inc.). RNA integrity was assessed by calculation of the percentage of fragments >200 nucleotides (DV200, Supplementary Table 3). Sequencing libraries were generated using 50 ng of total RNA and the QuantSeq 3′ mRNA-Seq Library Prep Kit FWD for Illumina (SKU: 015.96, Lexogen GmbH, Austria). Library amplification PCR cycles were determined using PCR Add-on Kit for Illumina (SKU: 020.96, Lexogen GmbH) and the individual libraries were amplified with 17 PCR cycles. Quality and quantity of the libraries were evaluated using the Quanti-iT PicoGreen dsDNA Assay Kit (P7589, Invitrogen) and the Bioanalyzer High Sensitivity DNA Analysis Kit (#5067-4626, Agilent Technologies, Inc.). 150 bp paired-end sequencing was performed on an Illumina HiSeq4000 platform (Illumina, Inc.). Lexogen QuantSeq 3′ library preparation was chosen for RNAseq analysis because it has the capability to generate high-quality gene expression data from low amounts (down to 10 pg) and/or compromised quality of total RNA. Both properties were expected from the small LCM-specimens used for RNAseq analysis.

RNAseq data analysis, differential expression analysis, gene set enrichment analysis (GSEA) and pathway responsive genes analysis (PROGENy)

Raw data, as well as preprocessed RNAseq data, are available from Gene Expression Omnibus (GEO accession number: GSE162795). Gene expression quantification was carried out by alignment of RNAseq reads to the mouse reference genome (Ensembl GRCm38 version 94) using the STAR aligner, followed by count quantification using the featureCounts of the Rsubreads R package (Dobin *et al.* 2013, Liao *et al.* 2014). Differential gene expression analysis was performed using methods implemented in the *DESeq2* R package (Love *et al.* 2014). Principal component analysis was carried out on variance stabilized read counts. Differential expression between proliferative

https://erc.bioscientifica.com
https://doi.org/10.1530/ERC-21-0019

lesions and corresponding normal tissue samples (PL vs NT) was performed with a paired design, while normal tissue vs normal control tissue and proliferative lesions vs normal control tissue (NT vs NCT, PL vs NCT), were analyzed in group comparisons controlled for sex and age. Genes with an absolute $\log_2$-fold change > 0.5 and an adjusted *P*-value < 0.1 were considered differentially expressed. The $\log_2$-fold change ($\log_2$-FC) and adjusted *P*-value thresholds were used solely to visualize the results of the differential expression analysis, but no functional interpretations were based on them. Gene set enrichment analysis (GSEA) was conducted in a pre-ranked mode using the $\log_2$-FC values obtained from DESeq2 (log-fold-change-shrinkage) for the ranking of the gene list using the fgsea R package (Sergushichev 2016, Powers *et al.* 2018). The Hallmark gene sets (n= 50), downloaded from Molecular Signature Database (http://software.broadinstitute.org/gsea/msigdb/index.jsp), plus additional thyroid pathogenesis-related or cancer-associated gene sets taken from the KEGG (n= 41) and Reactome (n= 23) gene set collections were used for enrichment testing (Supplementary Table 4). PROGENy analysis was carried out in order to test for a deregulation in eleven cancer relevant signal transduction pathways using transcriptomics data. In comparison to conventional pathway analysis methods (e.g. GSEA), PROGENy infers pathway activity based on consensus gene signatures obtained from perturbation experiments on protein level and constitutes the footprint on gene expression (Schubert *et al.* 2018).

qRT-PCR validation of RNAseq quantification

In addition to the technical quality control of the RNAseq data using FastQC, their validity was investigated by comparing the expression of eight randomly selected genes determined by RNAseq with that determined by qRT-PCR in all 27 samples. Four of the selected genes (CD36, HSP90AA1, IL1B, SERPINE1) were differentially expressed in one of the three comparisons carried out and four (ALAS1, LRP1, PLAU, THBS1) that did not show differential expression. Total RNA extracted from mouse tissue samples was processed and analyzed by qRT-PCR as described before (Krombach *et al.* 2019). Relative expression values were determined as delta CT-values to a reference gene matrix of 18S rRNA and beta-actin with efficiency correction via three different cDNA dilutions for each sample. Pearson correlation between RNAseq and qRT-PCR determined gene expression was used as a measure of concordance.

Clustering of samples using a literature-derived gene set

A literature-derived gene set consisting of 85 thyroid carcinogenesis- and thyroid cancer-associated genes, was utilized for hierarchical clustering of samples using correlation as distance measure (linkage 'complete') followed by visualization as heatmap including the cluster dendrogram using the pheatmap R package. The considered publications reported the genes to be associated with thyroid carcinogenesis and cancer and in greater detail with proliferation, metabolic deregulation, and immune signaling (Rusinek *et al.* 2011, Xing 2013, Giuliani *et al.* 2018, Vella & Malaguarnera 2018).

A subset of these genes was also present in the gene expression data set generated on the normal tissue and PTC tissue from the Ukranian-American cohort (UkrAM) of human individuals who were exposed to ionizing radiation as a consequence of the Chernobyl reactor accident (Abend *et al.* 2013). Their expression levels were compared to the expression data from the three histological groups generated in this study.

Results

Histological analysis reveals radiation-associated lesions

The histological analysis revealed nine mice with proliferative lesions in the thyroid (PL) out of 246 animals in total. PLs were exclusively present in the irradiated group while seven PLs were observed in the 24 months group (P=0.09) and two in the 18 months group (P=1). No significant difference with regard to the sex of animals was detected (male P=0.55; female P=0.18). Fisher's exact test for the frequency of PLs in the irradiated and non-irradiated group (9/164 exposed, 0/82 non-exposed) indicated a significant association between PL-occurrence and radiation exposure (P=0.03). Three out of nine alterations met the diagnostic criteria of an adenoma according to Capen's classification (Capen 2001). The remaining six cases were classified as follicular hyperplasia. Eventually, all nine lesions showed predominantly a papillary pattern, which is characterized by branching infoldings covered by a single-layered epithelium. While follicular hyperplasia is not well demarcated, adenomas often have a more complex architecture accompanied by encapsulation (Capen 2001). Since any signs of invasion of surrounding tissue or blood vessels were absent, none of the neoplastic lesions were classified as carcinoma.

https://erc.bioscientifica.com
https://doi.org/10.1530/ERC-21-0019

Immune cells (lymphocytes, neutrophils, plasma cells, and macrophages) were investigated, both, in irradiated and non-irradiated tissues and cells were counted to quantify the extent of infiltration. The highest density of immune cells was detected in proliferative tissue, followed by normal irradiated tissue and non-irradiated normal tissue. Microscopic images visualizing the location of the lesions within the thyroid glands, exemplary high-resolution images of the examined tissues, and the observed immune cell densities within the different tissues are provided in Supplementary Fig. 1. Statistically significant differences in immune cell densities (infiltration) were identified by ANOVA ($P<0.01$) and *post hoc* Tukey's test between proliferative and normal irradiated tissue (PL compared to NT, $P=0.01$) and between proliferative and non-irradiated normal tissue (PL compared to NCT, $P=0.001$). No significant difference between irradiated normal tissue and non-irradiated normal tissue was observed (NT compared to NCT, $P=0.23$, Supplementary Fig. 2). Sample information and histological classifications are summarized in Supplementary Tables 1 and 2.

qRT-PCR validation of RNAseq quantification

Pearson correlation coefficients ranged from 0.53 to 0.91 for seven out of the eight genes investigated, only the HSP90AA1 gene exhibited a correlation coefficient of 0.21 (Supplementary Table 5). These finding validate the 3′ RNAseq data, since only one gene detected with primers located near the 5′ end indicated low correlation.

Transcriptomic analysis points at deregulated pathways in normal tissue and proliferative lesions

Principal component analysis (PCA) of the RNAseq transcriptome data set exhibited grouping of the samples according to their histological classification, separating proliferative lesion samples (PL) very well from the corresponding normal tissue samples (NT) and normal control tissue samples (NCT). The separation of NT and NCT was less pronounced (Fig. 1C). Dimensionality reduction by multi-dimensional-scaling (MDS) and PCA using the top-500 variant genes in the data set are provided in Supplementary Fig. 3C and D, PC loadings are provided in Supplementary Tables 6 and 7. PROGENy analysis revealed an activated EGFR, MAPK and TNFa signal transduction in NT compared to NCT. The most prominent finding in PL compared to NT was a downregulated p53 signaling, while PL compared to NCT showed elevated proliferation-associated signaling (MAPK, PI3K, EGFR) and downregulated p53 signaling (Fig. 2A and Supplementary Table 8). With respect to $\log_2$-FC and false discovery rate (FDR), differential gene expression was least pronounced in NT compared to NCT (128 genes), followed by PL compared to NT (1355 genes), and PL compared to NCT (2379 genes), respectively (Fig. 2C and Supplementary Table 9). Common and specific genes for the three comparisons are visualized in Supplementary Fig. 4. Gene set enrichment analysis (GSEA) is visualized in Fig. 2D. All gene sets with an FDR < 0.1 in at least one out of the three comparisons were included into the plot. Mainly, activated immune signaling and a downregulated metabolic signaling in NT compared to NCT and activated proliferation-associated signaling and downregulated metabolic signaling in PT compared to NT was found (Fig. 2D) while PL compared to NCT showed increased proliferation-associated signaling.

Hierarchical clustering of histological groups based on literature-derived gene set

Hierarchical clustering analysis, based on the expression of the literature-derived and thyroid cancer-associated gene set (85 genes) resulted in three main clusters, separating the three histologically defined groups (Supplementary Fig. 3A). Additionally, the cluster affiliations were visualized in the PCA and MDS plots in Supplementary Fig. 3B, C and D. Thirty-one out of the 85 genes were differentially expressed (Supplementary Table 9). Mouse expression data were compared to human expression data using the microarray expression data set of thyroid cancers developed in the UkrAm cohort (Tronko *et al.* 2006). The expression levels of 26 out of the 31 differentially expressed genes were also present in the data set on human PTC. Differential expression of 14 out of these 26 genes in the human data, indicates their relevance in thyroid cancer/carcinogenesis in human and mouse tissue and the relevance of the studied tissues as a model for thyroid carcinogenesis (Supplementary Figs 5 and 6).

Discussion

This study aimed to elucidate early stages of thyroid tumorigenesis by investigating histological and molecular changes in mouse thyroids derived from mice after one-time exposure to ionizing radiation (Dalke *et al.* 2018). Besides the finding presented in this study, Dalke *et al.*

https://erc.bioscientifica.com
https://doi.org/10.1530/ERC-21-0019

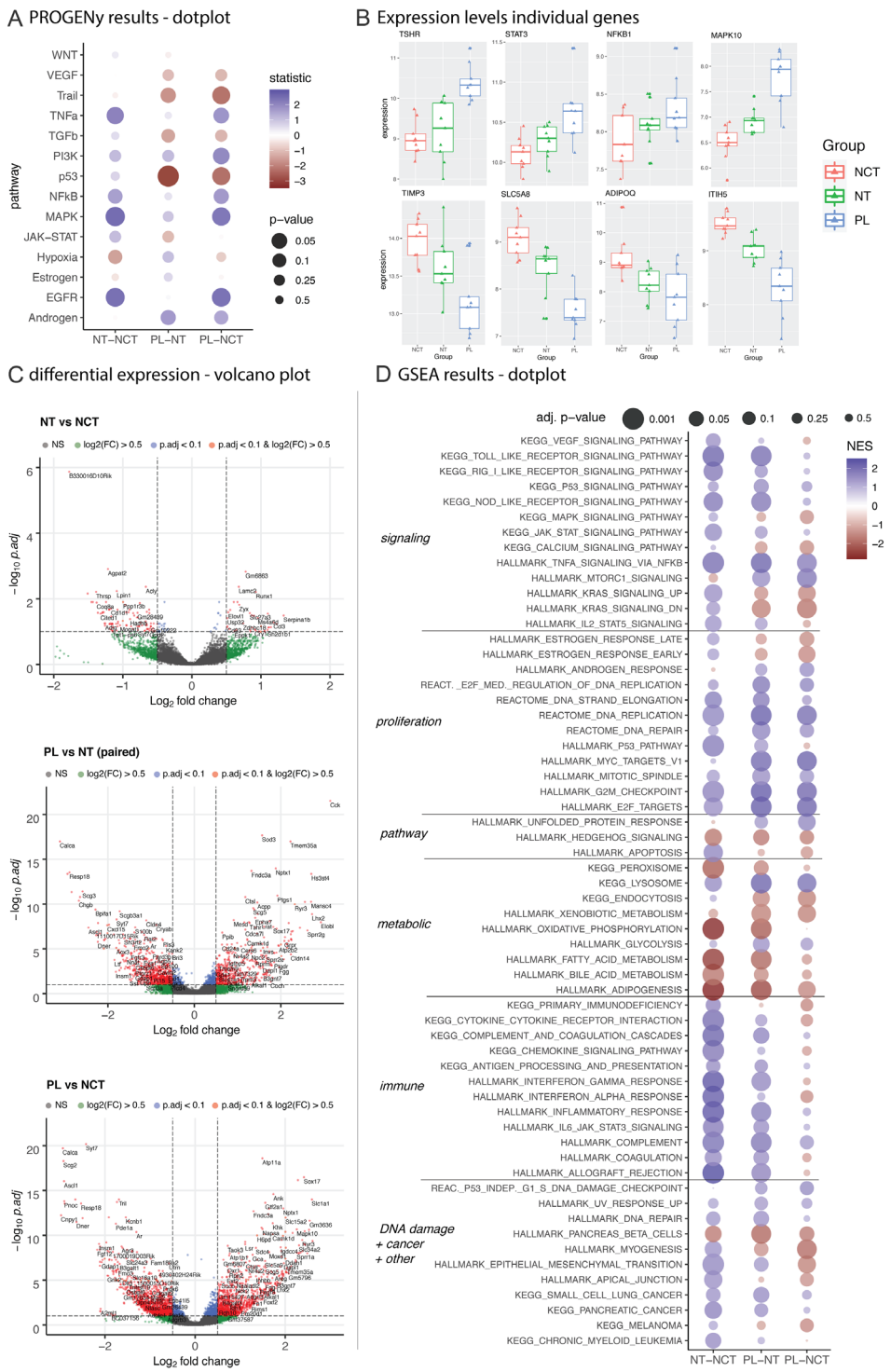

Figure 2

Transcriptomic analysis results. Panel A: Dot plot of PROGENy results: All pathways included in PROGENy were visualized. Dot size corresponds to signal strength (bigger is stronger), dot color reflects the direction of the deregulation (red: downregulated, blues: upregulated). Panel B: Box plots of gene expression (vst-counts/DESeq2) for a set of eight selected genes in the three histological groups. Panel C: Volcano plot of differential gene expression analysis. Panel D: Dot plot of gene set enrichment analysis (GSEA) results. Dot size corresponds to −log2(adj-*P*-value) (lager dot = smaller adj-*P*-value), dot color reflects the normalized enrichment score (NES) (red: downregulated, blue: upregulated). NCT, histologically normal tissue from non-exposed mice; NT, histologically normal tissue from exposed mice that harbor proliferative lesions; PL, proliferative lesions tissue from exposed mice. A full color version of this figure is available at https://doi.org/10.1530/ERC-21-0019.

https://erc.bioscientifica.com
https://doi.org/10.1530/ERC-21-0019

reported an association of one-time exposure to ionizing radiation with increased body weight, reduced survival rates and a dose-dependent association with several other tumor types and eye lens opacity (Dalke *et al.* 2018).

Mouse models are a valid tool to study the molecular mechanisms underlying thyroid tumorigenesis since it has been shown that large biological and histological similarities between human thyroid and mouse thyroid exist (Perlman 2016). However, the definitions of pre-neoplastic and neoplastic lesions diverge (Boorman 1995, Capen 2001, DeLellis 2004, Baloch & LiVolsi 2018). The different histological phenotypes and their histopathological classifications make a comparative diagnosis between the different cancer entities in mice and humans challenging. In this study, tissue samples were examined on the basis of Capen's International Classification of Rodent Tumors (Capen 2001), which does not distinguish between the different histological entities. Therefore, a comparative investigation of a specific cancer entity was not possible. Instead, we focused on early molecular processes of thyroid tumorigenesis that occurred in histologically normal and aberrant mouse thyroid tissues. While tumor initiation, promotion and progression in murine thyroids starts with proliferative lesions (e.g. hyperplasia), followed by follicular adenoma, which subsequently progress to follicular thyroid carcinoma, in humans it is more complex and is reflected by different thyroid carcinoma subtypes (Boorman 1995, Capen 2001, DeLellis 2004).

Comprehensive histological examination of 164 exposed and 82 non-exposed thyroids revealed neoplastic alterations exclusively in exposed mice, which is in line with multiple previous studies reporting ionizing radiation as one of the major risk factors for the development of thyroid carcinoma (Cardis *et al.* 2005, Ron 2007, Williams 2008, Zablotska *et al.* 2008, Mullenders *et al.* 2009, Furukawa *et al.* 2013, La Vecchia *et al.* 2015). While adenomas were identified within the exposed group, we did not observe any carcinoma in our study. This might be due to the limited life span of a mouse and the fact that the experiment was terminated at 24 months, which might not allow full progression of the carcinogenic process. These observations might reflect the widely acknowledged stepwise model of progression to cancer, in which the accumulation of mutations or other events leads to successive clonal expansion and aberrant phenotypes (Martincorena & Campbell 2015, Laconi *et al.* 2020). Barrett's esophagus is one prominent example of a precursor lesion on the road to malignancy, where a metaplasia-dysplasia-carcinoma sequence seems to be proven (Weaver *et al.* 2014). Although, we did not perform mutation typing, our findings support the stepwise model concept at the transcriptome and functional levels and provide insights for the poorly studied area of precancerous thyroid lesions.

It is, generally, accepted that inflammation is linked to cancer development (Mantovani *et al.* 2008). In thyroid cancer, the inflammatory tumor microenvironment, containing immune cells and mediators like chemokines, plays a central role in the carcinogenesis and is among the hallmarks of cancer (Hanahan & Weinberg 2011, Yapa *et al.* 2017). Tumor microenvironment as mutation promoter is discussed as potential driver of field cancerization of various cancer entities (Curtius *et al.* 2018). Although no acute inflammation was observed in the examined tissues, the number of immune cells present in the different histological groups steadily increased from normal control tissue (NCT), to normal tissue (NT), to proliferative lesions (PL) (Supplementary Fig. 2). The elevated immune cell numbers in NT and PL tissues potentially indicate deregulated chemokine expression that triggers physiologic changes and immune responses by the recruitment of specific immune cell populations to the tissue sites. Neoplastic thyroid cells have the ability to alter the chemokine system for their own benefit by influencing immune cell recruitment into the tumor microenvironment, thereby affecting multiple aspects of thyroid cancer progression (Yapa *et al.* 2017). These findings integrate well with elevated immune signaling in NT and PL tissues as shown by RNAseq analysis (GSEA and PROGENy) and potentially explain the increased numbers of immune cells in these tissues (Fig. 2 and Supplementary Fig. 2).

In order to analyze the histologically defined tissue regions on molecular level, we established a technically challenging workflow: first, we collected the cells forming the tissue regions of interest (PL, NT, NCT) from the tissue sections by LCM prior to extraction of total RNA from these comparably small numbers of cells, followed by high-quality RNA-sequencing library generation and RNA sequencing. Transcriptomic data were used to delineate molecular changes in histologically normal thyroid tissue (NT) and adjacent proliferative lesions that underwent a tumorigenic process (PL). Normal control tissues of non-irradiated mice (NCT) without any histological aberrations in the entire thyroid were used as a reference. Although, the differential expression analysis between NT and NCT showed the lowest level of transcriptomic deregulation within the three conducted differential expression analysis (log_2-FC, adjusted-*P*-value, Volcano plots, Fig. 2B),

https://erc.bioscientifica.com
https://doi.org/10.1530/ERC-21-0019

the deregulation was significantly functionally associated with tumorigenesis by PROGENy and GSEA. Despite the different concepts of functional association of transcriptomic deregulation in PROGENy and GSEA, the derived results integrate well and are biologically plausible in the context of the study.

The PROGENy results fit the concept of a progression model while the level of deregulation accumulates from healthy, histologically normal tissue (NCT) to histologically normal tissue with a deregulated molecular phenotype, that progresses further into tissue with histological abnormalities (PL). As an example (Fig. 2A), the p53-signaling was weakly upregulated in NT compared to NCT and strongly downregulated in PL compared to NT, resulting in less pronounced downregulation in PL compared to NCT. Contrarily, MAPK-signaling was highly upregulated in NT compared to NCT and PL compared to NCT, but did not show a difference in PL compared to NT. These observations allow the interpretation that the apoptotic processes mediated by p53 prevented the NT tissues that already showed an activated MAPK response, from excessive proliferation (which would be histologically visible), while the activated MAPK response potentially led to excessive proliferation in PL, were the p53 associated apoptosis is downregulated and cannot 'counter-act' the MAPK signaling. Observations for the NF-κB response are qualitatively identical and integrate well with this interpretation (Fig. 2A). Additionally, Pi3K signaling is activated in NT and PL compared to NCT. PI3K deregulation was previously described in association with follicular thyroid carcinoma and with anaplastic thyroid carcinoma (ATC) in conjunction with a MAPK cascade deregulation (Xing 2013).

The most prominent GSEA findings (Fig. 2D) in the comparison between NT and NCT are the elevated immune response signaling, comprised of gene sets representing allograft rejection, interferon alpha/gamma response, inflammatory response and TNFa via NF-κB signaling and confirm the PROGENY results that show an activated TNFa and NF-κB response in NT compared to NCT.

The NF-κB signaling pathway is one potential link between cancer and inflammation in thyroid carcinogenesis and a proven common mechanism to activate cell survival, proliferation and differentiation, contributing to tumor progression (Karin 2009, Li *et al.* 2013). It is interesting to note that, NF-κB signaling might either promote tumor growth by activating cell proliferation and angiogenesis or acts anti-tumorigenically by triggering an immune response and the attraction of immune cells (Pacifico *et al.* 2004, Pires *et al.* 2018). This could further explain the elevated proliferation-associated signaling on molecular level, without the presence of histological aberrations in NT tissues. Negatively enriched gene sets in the comparison of NT with NCT were exclusively associated with metabolic processes (Fig. 2D). These findings integrate well with the recently reported emerging role of the insulin receptor in the context of carcinogenesis of several malignant diseases including thyroid cancer (Vella & Malaguarnera 2018).

Consistently, proliferative lesions (PL) compared to the adjacent normal tissues (NT) showed strongly activated proliferation-associated processes, along with increased signals for immune-associated gene sets, while the immune-associated deregulation was not as strong as in NT compared to NCT. From these findings, we concluded that molecular deregulations leading to an activation of the immunologic processes, such as metabolic processes, are already present in histologically normal tissues (NT). Metabolic processes in PL-NCT and NT-NCT show similar regulation patterns, including the peroxisome- and lysosome-associated gene that suggest differences in the metabolic transport processes in NT and PL tissues.

Additionally, KRAS signaling was deregulated in all three comparisons, while the signal appears fundamentally different in PL-NT and PL-NCT compared NT-NCT (Fig. 2D), potentially indicating a mutation in this pathway. KRAS, along with other RAS mutations, was described in association with deregulated cell proliferation in multiple cancer entities (Xing 2016).

Confirmatory studies on protein level and data on the BRAF V600E mutation status, genomic rearrangements, such as RET/PTC rearrangements and PAX8-PPARG fusions, which are frequently described in thyroid carcinoma would be desirable to further support the conclusions drawn from this study. However, this was not feasible due to the limited amounts of tissue derived from the small LCM-specimen.

While multiple studies discuss the effect of specific genes on a single process of thyroid carcinogenesis, we aimed at an integrated analysis by applying a hierarchical clustering approach on the transcriptomic data. Using 85 thyroid carcinogenesis and thyroid cancer-associated genes derived from the literature (Supplementary Table 10, functional grouping and citations), separation into three defined histological groups was achieved. This suggests that carcinogenic processes are already ongoing within the proliferative lesions of this study thus representing early stages of thyroid tumorigenesis. The expression levels in the three histologic groups of multiple thyroid

https://erc.bioscientifica.com
https://doi.org/10.1530/ERC-21-0019

carcinogenesis- and cancer-associated genes indicate that the analyzed tissues represent sequential stages of molecular and histologic transformation in thyroid tumorigenesis. Increasing expressions from NCT, via NT, to PL for the thyroid tumor-promoting genes TSHR, IDH1, NFKB1, HIF1AN, STAT3, TPO, TRP53, TMEM173 (STING), IGF1, MAPK10 and decreasing expressions for tumor-suppressing genes such as SLC5A8, TIMP3, ITIH5, PCSK2 were observed (Fig. 2B, Supplementary Fig. 5 and Supplementary Table 10). This further underlines that the PL tissues might represent early stages during thyroid tumorigenesis and that histologically normal tissues (NT) already show molecular deregulations pointing to the development of thyroid cancer.

Additionally, 26 out of the 31 differentially expressed genes in the 85-gene set that were present in the human UkrAm gene expression data set showed similar regulation patterns and significant differential expression between normal tissue and tumor tissue (PTC) samples compared to the expression data generated within this study (Supplementary Figs 5 and 6). This indicates that these genes that are known to be deregulated during the early phases of the carcinogenic process remain to be deregulated in human PTC and confirm the herein studied tissues as a relevant model for the early phases of thyroid tumorigenesis.

Our study design, which was also determined by limited availability of biomaterial, does not allow for a clear discrimination between potential radiation effects and early processes toward proliferative thyroid lesions at the transcriptome level. Nevertheless, regardless of the trigger we were able to detect functionally relevant deregulation that is conclusive with respect to the affected molecular processes and integrates well with findings within the present and previous studies on thyroid carcinogenesis and early-stage processes of several other cancer entities.

Conclusion

In conclusion, we hypothesize that the histologically normal tissues (NT), which contain no macroscopically detectable abnormalities, represent a very early stage in thyroid carcinogenesis and will further progress to thyroid hyperplasia, followed by thyroid adenoma and potentially by thyroid carcinoma. While NT tissues exhibit histologically normal structures, the molecular footprint compared to normal control tissues (NCT) already indicates an initiation of carcinogenic processes. These findings integrate well with the proposed multi-step model and the fetal cell carcinogenesis model as discussed in Zane *et al.* (2016). Potential clinical implication might be a refined thyroid cancer diagnosis, which is currently carried out by fine needle biopsy followed by cytologic classification. Further investigation of thyroid tissues with normal histology and deregulated molecular levels are necessary in order to develop a molecular signature or marker for implementation in routine clinical diagnostics.

Supplementary materials
This is linked to the online version of the paper at https://doi.org/10.1530/ERC-21-0019.

Declaration of interest
The authors declare that there is no conflict of interest that could be perceived as prejudicing the impartiality of the research reported.

Funding
The INSTRA project is funded by the Bundesministerium für Bildung und Forschung (BMBF) (grant number 02NUK045A), while no influence or suggestions were made with respect to the collection, analysis and interpretation of data, the writing of the report and the decision to submit the article for publication.

Ethical approval
All applicable international, national and/or institutional guidelines for the care and use of animals were followed. In particular, the study was approved by the government of Upper Bavaria (Az. 55.2-1-54-2532-161-12).

Author contribution statement
K Unger and M Selmansberger contributed equally to this work.

Acknowledgements
The authors thank Laura Dajka, Claire Innerlohinger, Aaron Selmeier, Isabella Zagorski and Steffen Heuer for their excellent technical support. Public availability of RNAseq data: GEO accession number GSE162795.

References

Abend M, Pfeiffer RM, Ruf C, Hatch M, Bogdanova TI, Tronko MD, Hartmann J, Meineke V, Mabuchi K & Brenner AV 2013 Iodine-131 dose-dependent gene expression: alterations in both normal and tumour thyroid tissues of post-Chernobyl thyroid cancers. *British*

Journal of Cancer **109** 2286–2294. (https://doi.org/10.1038/bjc.2013.574)

Baloch ZW & LiVolsi VA 2018 Special types of thyroid carcinoma. *Histopathology* **72** 40–52. (https://doi.org/10.1111/his.13348)

Boorman GA & Hailey JR 1995 Preneoplastic and neoplastic lesions of the rat and mouse thyroid. In *Pathology of Neoplasia and Preneoplasia in Rodents*. Eds P Bannasch & W Gossner. Stuttgart, New York: Schattauer.

Brown TC, Juhlin CC, Healy JM, Prasad ML, Korah R & Carling T 2014 Frequent silencing of RASSF1A via promoter methylation in follicular thyroid hyperplasia: a potential early epigenetic susceptibility event in thyroid carcinogenesis. *JAMA Surgery* **149** 1146–1152. (https://doi.org/10.1001/jamasurg.2014.1694)

Cahoon EK, Nadyrov EA, Polyanskaya ON, Yauseyenka VV, Veyalkin IV, Yeudachkova TI, Maskvicheva TI, Minenko VF, Liu W, Drozdovitch V, *et al*. 2017 Risk of thyroid nodules in residents of belarus exposed to Chernobyl fallout as children and adolescents. *Journal of Clinical Endocrinology and Metabolism* **102** 2207–2217. (https://doi.org/10.1210/jc.2016-3842)

Capen C 2001 Endocrine system-thyroid gland. In *International Classification of Rodent Tumours*. *The Mouse*. Ed U Mohr. Springer.

Cardis E, Kesminiene A, Ivanov V, Malakhova I, Shibata Y, Khrouch V, Drozdovitch V, Maceika E, Zvonova I, Vlassov O, *et al*. 2005 Risk of thyroid cancer after exposure to 131I in childhood. *Journal of the National Cancer Institute* **97** 724–732. (https://doi.org/10.1093/jnci/dji129)

Colamaio M, Puca F, Ragozzino E, Gemei M, Decaussin-Petrucci M, Aiello C, Bastos AU, Federico A, Chiappetta G, Del Vecchio L, *et al*. 2015 miR-142-3p down-regulation contributes to thyroid follicular tumorigenesis by targeting ASH1L and MLL1. *Journal of Clinical Endocrinology and Metabolism* **100** E59–E69. (https://doi.org/10.1210/jc.2014-2280)

Curtius K, Wright NA & Graham TA 2018 An evolutionary perspective on field cancerization. *Nature Reviews: Cancer* **18** 19–32. (https://doi.org/10.1038/nrc.2017.102)

Dalke C, Neff F, Bains SK, Bright S, Lord D, Reitmeir P, Rossler U, Samaga D, Unger K, Braselmann H, *et al*. 2018 Lifetime study in mice after acute low-dose ionizing radiation: a multifactorial study with special focus on cataract risk. *Radiation and Environmental Biophysics* **57** 99–113. (https://doi.org/10.1007/s00411-017-0728-z)

DeLellis RA 2004 Tumors of the thyroid and parathyroid. In *World Health Organization (WHO) Classification of Tumors-Pathology and Genetics of Tumours of Endocrine Organs*. Eds RA Delellis, RV Lloyd, PV Heitz & C Eng. Lyon: IARC Press.

Dobin A, Davis CA, Schlesinger F, Drenkow J, Zaleski C, Jha S, Batut P, Chaisson M & Gingeras TR 2013 STAR: ultrafast universal RNA-seq aligner. *Bioinformatics* **29** 15–21. (https://doi.org/10.1093/bioinformatics/bts635)

Efanov AA, Brenner AV, Bogdanova TI, Kelly LM, Liu P, Little MP, Wald AI, Hatch M, Zurnadzy LY, Nikiforova MN, *et al*. 2018 Investigation of the relationship between radiation dose and gene mutations and fusions in post-Chernobyl thyroid cancer. *Journal of the National Cancer Institute* **110** 371–378. (https://doi.org/10.1093/jnci/djx209)

Furukawa K, Preston D, Funamoto S, Yonehara S, Ito M, Tokuoka S, Sugiyama H, Soda M, Ozasa K & Mabuchi K 2013 Long-term trend of thyroid cancer risk among Japanese atomic-bomb survivors: 60 years after exposure. *International Journal of Cancer* **132** 1222–1226. (https://doi.org/10.1002/ijc.27749)

Giuliani C, Bucci I & Napolitano G 2018 The role of the transcription factor nuclear factor-kappa B in thyroid autoimmunity and cancer. *Frontiers in Endocrinology* **9** 471. (https://doi.org/10.3389/fendo.2018.00471)

Hanahan D & Weinberg RA 2011 Hallmarks of cancer: the next generation. *Cell* **144** 646–674. (https://doi.org/10.1016/j.cell.2011.02.013)

Jokinen MP & Botts S 1994 *Tumours of the Thyroid Gland*. IARC Scientific Publications, pp. 565–594.

Jung SH, Kim MS, Jung CK, Park HC, Kim SY, Liu J, Bae JS, Lee SH, Kim TM, lee SH, *et al*. 2016 Mutational burdens and evolutionary ages of thyroid follicular adenoma are comparable to those of follicular carcinoma. *Oncotarget* **7** 69638–69648. (https://doi.org/10.18632/oncotarget.11922)

Karin M 2009 NF-kappaB as a critical link between inflammation and cancer. *Cold Spring Harbor Perspectives in Biology* **1** a000141. (https://doi.org/10.1101/cshperspect.a000141)

Kazakov VS, Demidchik EP & Astakhova LN 1992 Thyroid cancer after Chernobyl. *Nature* **359** 21. (https://doi.org/10.1038/359021a0)

Kondo T, Ezzat S & Asa SL 2006 Pathogenetic mechanisms in thyroid follicular-cell neoplasia. *Nature Reviews: Cancer* **6** 292–306. (https://doi.org/10.1038/nrc1836)

Krombach J, Hennel R, Brix N, Orth M, Schoetz U, Ernst A, Schuster J, Zuchtriegel G, Reichel CA, bierschenk S, *et al*. 2019 Priming anti-tumor immunity by radiotherapy: dying tumor cell-derived DAMPs trigger endothelial cell activation and recruitment of myeloid cells. *Oncoimmunology* **8** e1523097. (https://doi.org/10.1080/2162402X.2018.1523097)

La Vecchia C, Malvezzi M, Bosetti C, Garavello W, Bertuccio P, Levi F & Negri E 2015 Thyroid cancer mortality and incidence: a global overview. *International Journal of Cancer* **136** 2187–2195. (https://doi.org/10.1002/ijc.29251)

Laconi E, Marongiu F & Degregori J 2020 Cancer as a disease of old age: changing mutational and microenvironmental landscapes. *British Journal of Cancer* **122** 943–952. (https://doi.org/10.1038/s41416-019-0721-1)

Li X, Abdel-Mageed AB, Mondal D & Kandil E 2013 The nuclear factor kappa-B signaling pathway as a therapeutic target against thyroid cancers. *Thyroid* **23** 209–218. (https://doi.org/10.1089/thy.2012.0237)

Liao Y, Smyth GK & Shi W 2014 featureCounts: an efficient general purpose program for assigning sequence reads to genomic features. *Bioinformatics* **30** 923–930. (https://doi.org/10.1093/bioinformatics/btt656)

Love MI, Huber W & Anders S 2014 Moderated estimation of fold change and dispersion for RNA-seq data with DESeq2. *Genome Biology* **15** 550. (https://doi.org/10.1186/s13059-014-0550-8)

Mantovani A, Allavena P, Sica A & Balkwill F 2008 Cancer-related inflammation. *Nature* **454** 436–444. (https://doi.org/10.1038/nature07205)

Martincorena I & Campbell PJ 2015 Somatic mutation in cancer and normal cells. *Science* **349** 1483–1489. (https://doi.org/10.1126/science.aab4082)

Morrogh M, Olvera N, Bogomolniy F, Borgen PI & King TA 2007 Tissue preparation for laser capture microdissection and RNA extraction from fresh frozen breast tissue. *BioTechniques* **43** 41–42, 44, 46 passim. (https://doi.org/10.2144/000112497)

Mullenders L, Atkinson M, Paretzke H, Sabatier L & Bouffler S 2009 Assessing cancer risks of low-dose radiation. *Nature Reviews: Cancer* **9** 596–604. (https://doi.org/10.1038/nrc2677)

Nikiforov YE 2006 Radiation-induced thyroid cancer: what we have learned from Chernobyl. *Endocrine Pathology* **17** 307–317. (https://doi.org/10.1007/s12022-006-0001-5)

Nikiforov YE & Nikiforova MN 2011 Molecular genetics and diagnosis of thyroid cancer. *Nature Reviews. Endocrinology* **7** 569–580. (https://doi.org/10.1038/nrendo.2011.142)

Nikiforova MN & Nikiforov YE 2008 Molecular genetics of thyroid cancer: implications for diagnosis, treatment and prognosis. *Expert Review of Molecular Diagnostics* **8** 83–95. (https://doi.org/10.1586/14737159.8.1.83)

Pacifico F, Mauro C, Barone C, Crescenzi E, Mellone S, Monaco M, Chiappetta G, Terrazzano G, Liguoro D, Vito P, *et al*. 2004 Oncogenic

and anti-apoptotic activity of NF-kappa B in human thyroid carcinomas. *Journal of Biological Chemistry* **279** 54610–54619. (https://doi.org/10.1074/jbc.M403492200)

Perlman RL 2016 Mouse models of human disease: an evolutionary perspective. *Evolution, Medicine, and Public Health* **2016** 170–176. (https://doi.org/10.1093/emph/eow014)

Pires BRB, Silva RCMC, Ferreira GM & Abdelhay E 2018 NF-kappaB: two sides of the same coin. *Genes* **9** 24. (https://doi.org/10.3390/genes9010024)

Powers RK, Goodspeed A, Pielke-Lombardo H, Tan AC & Costello JC 2018 GSEA-InContext: identifying novel and common patterns in expression experiments. *Bioinformatics* **34** i555–i564. (https://doi.org/10.1093/bioinformatics/bty271)

Ron E 2007 Thyroid cancer incidence among people living in areas contaminated by radiation from the Chernobyl accident. *Health Physics* **93** 502–511. (https://doi.org/10.1097/01.HP.0000279018.93081.29)

Ron E, Lubin JH, Shore RE, Mabuchi K, Modan B, Pottern LM, Schneider AB, Tucker MA & Boice Jr JD 1995 Thyroid cancer after exposure to external radiation: a pooled analysis of seven studies. *Radiation Research* **141** 259–277. (https://doi.org/10.2307/3579003)

Rusinek D, Szpak-Ulczok S & Jarzab B 2011 Gene expression profile of human thyroid cancer in relation to its mutational status. *Journal of Molecular Endocrinology* **47** R91–R103. (https://doi.org/10.1530/JME-11-0023)

Schubert M, klinger B, klünemann M, sieber A, uhlitz F, sauer S, garnett MJ, blüthgen N & saez-rodriguez J 2018 Perturbation-response genes reveal signaling footprints in cancer gene expression. *Nature Communications* **9** 20. (https://doi.org/10.1038/s41467-017-02391-6)

Sedaghati M & Kebebew E 2019 Long noncoding RNAs in thyroid cancer. *Current Opinion in Endocrinology, Diabetes, and Obesity* **26** 275–281. (https://doi.org/10.1097/MED.0000000000000497)

Sergushichev A 2016 An algorithm for fast preranked gene set enrichment analysis using cumulative statistic calculation. *bioRxiv* [epub]. (https://doi.org/10.1101/060012)

Sponziello M, Lavarone E, Pegolo E, Di Loreto C, Puppin C, Russo MA, Bruno R, Filetti S, Durante C, Russo D, *et al*. 2013 Molecular differences between human thyroid follicular adenoma and carcinoma revealed by analysis of a murine model of thyroid cancer. *Endocrinology* **154** 3043–3053. (https://doi.org/10.1210/en.2013-1028)

Tronko MD, Howe GR, Bogdanova TI, Bouville AC, Epstein OV, Brill AB, Likhtarev IA, Fink DJ, Markov VV, Greenebaum E, *et al*. 2006 A cohort study of thyroid cancer and other thyroid diseases after the chornobyl accident: thyroid cancer in Ukraine detected during first screening. *Journal of the National Cancer Institute* **98** 897–903. (https://doi.org/10.1093/jnci/djj244)

Vella V & Malaguarnera R 2018 The emerging role of insulin receptor isoforms in thyroid cancer: clinical implications and new perspectives. *International Journal of Molecular Sciences* **19** 3814. (https://doi.org/10.3390/ijms19123814)

Vogelstein B & Kinzler KW 1993 The multistep nature of cancer. *Trends in Genetics* **9** 138–141. (https://doi.org/10.1016/0168-9525(93)90209-z)

Weaver JMJ, Ross-Innes CS, Shannon N, Lynch AG, Forshew T, Barbera M, Murtaza M, Ong CJ, Lao-Sirieix P, Dunning MJ, *et al*. 2014 Ordering of mutations in preinvasive disease stages of esophageal carcinogenesis. *Nature Genetics* **46** 837–843. (https://doi.org/10.1038/ng.3013)

Williams D 2008 Radiation carcinogenesis: lessons from Chernobyl. *Oncogene* **27** (Supplement 2) S9–S18. (https://doi.org/10.1038/onc.2009.349)

Wiltshire JJ, Drake TM, Uttley L & Balasubramanian SP 2016 Systematic review of trends in the incidence rates of thyroid cancer. *Thyroid* **26** 1541–1552. (https://doi.org/10.1089/thy.2016.0100)

Xing M 2005 BRAF mutation in thyroid cancer. *Endocrine Related Cancer* **12** 245–262. (https://doi.org/10.1677/erc.1.0978)

Xing M 2013 Molecular pathogenesis and mechanisms of thyroid cancer. *Nature Reviews: Cancer* **13** 184–199. (https://doi.org/10.1038/nrc3431)

Xing M 2016 Clinical utility of RAS mutations in thyroid cancer: a blurred picture now emerging clearer. *BMC Medicine* **14** 12. (https://doi.org/10.1186/s12916-016-0559-9)

Yapa S, Mulla O, Green V, England J & Greenman J 2017 The role of chemokines in thyroid carcinoma. *Thyroid* **27** 1347–1359. (https://doi.org/10.1089/thy.2016.0660)

Ye L, Zhou X, Huang F, Wang W, Qi Y, Xu H, Yang S, Shen L, Fei X, Xie J, *et al*. 2017 The genetic landscape of benign thyroid nodules revealed by whole exome and transcriptome sequencing. *Nature Communications* **8** 15533. (https://doi.org/10.1038/ncomms15533)

Zablotska LB, Bogdanova TI, Ron E, Epstein OV, Robbins J, Likhtarev IA, Hatch M, Markov VV, Bouville AC, Olijnyk VA, *et al*. 2008 A cohort study of thyroid cancer and other thyroid diseases after the Chornobyl accident: dose-response analysis of thyroid follicular adenomas detected during first screening in Ukraine (1998–2000). *American Journal of Epidemiology* **167** 305–312. (https://doi.org/10.1093/aje/kwm301)

Zane M, Scavo E, Catalano V, Bonanno M, Todaro M, De Maria R & Stassi G 2016 Normal vs cancer thyroid stem cells: the road to transformation. *Oncogene* **35** 805–815. (https://doi.org/10.1038/onc.2015.138)

Received in final form 10 February 2021
Accepted 12 February 2021
Accepted Manuscript published online 19 February 2021